



## Nortriptyline for smoking cessation: Release and human skin diffusion from patches

A. Melero<sup>a,b</sup>, T.M. Garrigues<sup>a,\*</sup>, M. Alós<sup>a</sup>, K.H. Kostka<sup>c</sup>, C.M. Lehr<sup>b</sup>, U.F. Schaefer<sup>b</sup>

<sup>a</sup> Department of Pharmacy and Pharmaceutics, Faculty of Pharmacy, University of Valencia, Av. Vicente Andrés Estellés, s/n, 46100-Burjassot, Valencia, Spain

<sup>b</sup> Biopharmaceutics and Pharmaceutical Technology, Saarland University, Campus, Building A4-1, D-66123 Saarbrücken, Germany

<sup>c</sup> Department of Plastic and Hand Surgery, Caritas-Hospital, Lebach, Germany

### ARTICLE INFO

#### Article history:

Received 30 March 2009

Received in revised form 15 May 2009

Accepted 25 May 2009

Available online 6 June 2009

#### Keywords:

Nortriptyline Hydrochloride

Patch

Transdermal delivery

Release

Smoke cessation

Tape-stripping

### ABSTRACT

The objective of this work was to develop a simple and inexpensive transdermal formulation containing Nortriptyline Hydrochloride (NTH) for smoking cessation support therapy. Hydroxypropyl-methylcellulose was chosen as polymer and a mixture of transdermal enhancers (selected from previous research) was incorporated. The formulations were characterised in terms of appearance, thickness, uniformity of NTH content, release and skin permeation. Release studies demonstrated controlled release for four formulations. Diffusion studies were performed through human heat separated epidermis (HHSE) using Franz Diffusion Cells (FDC). Patches provided different fluxes varying from  $20.39 \pm 7.09 \mu\text{g}/(\text{cm}^2 \text{ h})$  to  $256.19 \pm 94.62 \mu\text{g}/(\text{cm}^2 \text{ h})$ . The penetration profiles of NTH within the stratum corneum (SC) and deeper skin layers (DSL) were established after three administration periods (3 h, 6 h, and 24 h). Skin changes induced by the application of the patches were observed by confocal laser scanning microscopy (CLSM). The highest flux obtained would provide the recommended doses for smoke cessation support therapy (25–75 mg per day) with a  $2 \text{ cm} \times 2 \text{ cm}$  patch or a  $3.5 \text{ cm} \times 3.5 \text{ cm}$  patch, respectively, without skin damage evidence.

© 2009 Elsevier B.V. All rights reserved.

### 1. Introduction

Smokers are becoming more conscious about the impact of their addiction on their health and many of them are willing to quit. This trend has grown over the last years, in part because of more restrictive laws of many governments and in part because the growing evidence of side effects caused by the addition to tobacco. At present, smoking cessation therapies combine psychological advice with pharmacologic therapy. Among the pharmacologic therapy, two strategies have been described. The first one is based on nicotine administration to avoid the physical effects caused by the sudden removal of the drug, though smokers can become dependent on it. The second pharmacological therapy is focused on the depression symptoms observed after quitting, but it is still not well addressed. So that it is widely accepted that there is a need of improvement in the current therapies.

Considering antidepressants, Nortriptyline Hydrochloride (NTH) has been shown to be effective and safe (Stimmel, 1996), even though it has not been selected as first choice therapy because of its low oral bioavailability (between 30 and 50%) and side effects associated to plasma level fluctuations. These problems may cause

lack of compliance and possible failure of the therapy (Stimmel, 1996; Prohazka, 1998). Changing the administration route to transdermal, these drawbacks can be overcome as there is no first pass associated and patches are pharmaceutical dosage forms well accepted by patients. The main advantage that transdermal drug delivery possesses over oral dose regimens is avoiding the variability associated with the gastrointestinal tract (effects of pH, motility, and transit time or food intake) (Farahmand and Maibach, 2009).

Previous research has demonstrated that NTH can effectively diffuse through human heat separated epidermis (HHSE) with the aid of chemical enhancers (Melero et al., 2008), so that, transdermal administration of this drug should be possible with an optimised Transdermal Drug Delivery System (TDDS).

This work studied five NTH patches in order to select a formulation which could reach the target plasma levels with a comfortable size ( $50 \text{ cm}^2$  or less) and thickness (a maximum of 1 mm). Controlled release of drug to maintain plasma levels for an extended period of time was also desired. Penetration was characterised by Franz Diffusion Cells (FDC) experiences on HHSE, which is considered as the golden standard for transdermal drug delivery studies. Drug distribution profiles within the different skin layers have also been obtained using the Saarbruecken model. Both penetration studies can be used to ascertain the influence of the vehicle in the process. Finally, changes in the skin after application of the patches

\* Corresponding author. Tel.: +34963543323; fax: +34 96 354 4911.

E-mail address: [Teresa.garrigues@uv.es](mailto:Teresa.garrigues@uv.es) (T.M. Garrigues).

were assessed by confocal laser scanning microscopy (CLSM). All this information allows the selection of a NTH patch worth to be evaluated in a preclinical study.

## 2. Materials and methods

### 2.1. Materials

NTH (min. 98%), ethanol (absolute), lactic acid (LA) (min. 85%), propylene glycol (PG) (99%) and hydroxypropyl-methylcellulose (HPMC) (2910) were purchased from Sigma Chemical (Madrid, Spain). Oleic acid (OA) (65–88%) and polysorbate 80 (PS80) (Pharmacopoeia Grade) were obtained from Fluka (Buchs SG, Switzerland). The rest of chemicals were of high-performance liquid chromatography (HPLC) analytical grade. Teflon filter Minisart, pore size 0.2 mm was purchased from Sartorius (Goettingen, Germany). Plastibase® was purchased from Heyden GmbH (Muenchen, Germany). A Cryomicrotome HR Mark II, model 1978, SLEE (Mainz, Germany) was used for the cryosection of deeper skin layers. Multi-film kristall-klar (Beiersdorf, Hamburg, Germany) was used for the tape-stripping experiments.

### 2.2. Determination of NTH

The samples were analyzed by a validated reverse phase HPLC method (Ghahramani and Lennard, 1996). The equipment consisted of a Hewlett-Packard joint 1050 (Barcelona, Spain) with ultraviolet detection ( $\lambda = 254$  nm) and a Kromasil C-18 (150 mm  $\times$  3.9 mm, 4  $\mu$ m, Scharlab S.L. Barcelona, Spain) column. A mixture of acetonitrile/phosphoric acid solution (1/15 M, pH 3.00) at 50/50 (v/v) was eluted at 1.0 ml min<sup>-1</sup>, 22 °C. The specifications of the method were within range during the analysis (relative error lower than 9.6%, inter-day variation coefficient below 2.7%). The injection volume was 50  $\mu$ l. The HPLC method was validated for accuracy (9.6% as the highest relative error obtained in the concentration range), precision (2.7% as the highest variation coefficient) and linearity over the concentration range analyzed ( $r^2 > 0.999$ ). The limit of quantification was 50 ng/mL.

### 2.3. Preparation of NHT film formulations

Five different formulations containing NTH and using HPMC as film forming polymer were prepared. Their composition is shown in Table 1. Two patches from previous studies were added as control (P1 and P2). As can be observed, the main difference between A and B is the presence or absence of PS80. C is similar to B except for the absence of OA. D has the same composition than B but 8% NTH. Formulation E, containing 10% of NTH, presents 1% HPMC because drug precipitation occurred with 2% concentration.

Solvents were weighed in the established ratio and NTH was dissolved in the solution under stirring, with a speed of 500 rpm. OA was incorporated at a concentration of 1% (if present) and the mixtures were stirred overnight. HPMC was weighted and slowly incorporated to the mixture increasing the stirring speed to 800 rpm. Once it was fully hydrated and gel consistence was

**Table 1**  
Composition of the different formulations assayed.

(%)	Film A	Film B	Film C	Film D	Film E	P1	P2
NTH	4	4	4	8	10	2	2
EtOH	30	30	30	30	30	30	30
PG	30	30	30	30	30	30	30
OA	1	1	–	1	1	1	1
PS80	–	1	1	1	1	–	1
HPMC	2	2	2	2	1	2	2
H <sub>2</sub> O	33	32	33	28	27	35	34

obtained, 20 g of the mixture were placed on a 95 mm diameter Petri-dish and dried at 50 °C over a heating plate under the extractor hood for 6 h.

### 2.4. Physical–chemical characteristics of the prepared films

#### 2.4.1. Odour and transparency

Odourlessness of the films was evaluated by sensory evaluation perceived by human nose of six volunteers.

Transparency was evaluated by comparing the patches with a transparent polyester film in a black background with daylight.

#### 2.4.2. Film thickness

The thickness of the films was measured at six different points using a micrometer, tactile probe 10B (Heidenhein, Traunreut, Germany), with an accuracy of  $\pm 1$   $\mu$ m. Mean values were calculated and are reported.

#### 2.4.3. Film NTH content uniformity

Three circles of the prepared films were cut with a 9 mm diameter punch. The circles were weighted and solved in a known volume of phosphate buffer 1/15 M, pH 5.5. The content of NTH was analyzed by HPLC as described.

#### 2.4.4. In vitro drug release study

The release of drug was examined using static Franz Diffusion Cells (FDC) of 15 mm diameter (type 4G-O1-00-20, Perme Gear, Riegelsville, PA, USA). The receptor compartment was filled with 12 ml phosphate buffer solution (1/15 M, pH 5.5) free of air bubbles and a 15-mm diameter circle of dialysis membrane was placed between donor and receptor compartment. As it has been demonstrated, this membrane was considered non-rate limiting for the drug diffusion (Melero et al., 2008). 100  $\mu$ l of phosphate buffer (1/15 M, pH 5.5) was placed over the membrane in order to moisture it and assure the adhesion of the film. Finally, a 13 mm diameter film circle was placed on top of the wetted membrane in the donor compartment and the donor compartment was sealed with Parafilm® and aluminum foil. The FDC were placed in a 32 °C tempered oven and stirred at 500 rpm. Samples of 400  $\mu$ l were collected after 0.25 h, 0.5 h, 0.75 h, 1 h, 1.5 h, 2 h, 4 h, 6 h, and 24 h. The same volume of fresh buffer was replaced in the receptor compartment after sampling. Concentration of NTH in the samples was quantified by HPLC as described above. Five replicates were carried out for each condition.

Cumulative amounts of NTH vs time were plotted. The release was characterised by fitting the power law equation (Eq. (1)) to data (Siepmann and Peppas, 2001):

$$\frac{Q_t}{Q_{inf}} = k_d \cdot t^n \quad (1)$$

where  $Q_t$  and  $Q_{inf}$  are the absolute cumulative amount of drug released at time  $t$  and the experimentally determined amount present in the disc, respectively;  $k_d$  is a constant that includes structural and geometric characteristics of the device and  $n$  is the release exponent, indicative of the mechanism of the process.

Data were also fitted to the classical first order equation. The non-linear regression program SigmaPlot 8.0® was used. The goodness of fits were characterised by the correlation coefficient and Akaike criterion, which was also used as selection criterion.

### 2.5. In vitro skin diffusion studies

#### 2.5.1. Preparation of human heat separated epidermis (HHSE)

Human skin samples were obtained from cosmetic surgery performed in the hospital Caritaskrankenhaus (Lebach, Germany). Abdominal skin from one anonymous female patient has been used

for these diffusion experiments, to avoid any inter-individual variability that could mask the studied parameters (Dragevic-Ciric et al., 2009; Morris et al., 2009). The fatty tissue was removed with a scalpel and the skin was cut into 10 cm × 10 cm pieces. They were stored in a freezer at  $-26^{\circ}\text{C}$  for a maximum time of three months. Epidermis was separated from the rest of the skin by a heat-separation technique developed by Kligmann in 1963 (Kligman and Christophers, 1963). Discs of 25 mm diameter were cut with a punch and submerged in  $60^{\circ}\text{C}$  tempered water for 45 s. Epidermis was then removed from the dermis with the help of a forceps and stored in physiologic solution till samples were placed on the FDC.

#### 2.5.2. Franz Diffusion Cells set-up

All skin experiments were carried out as described in Section 2.4.3 with the exception that HHSE was used in combination with the dialysis membrane. Furthermore, the cells were equilibrated for 1 h to complete the hydration of HHSE. After removing air bubbles, 100  $\mu\text{l}$  of the same phosphate buffer was placed over the membrane in order to moisture it and assure the adhesion of the film. Finally, a 13 mm diameter film disc was placed on top of the HHSE and the donor compartment was covered with Parafilm<sup>®</sup> and aluminum foil. Samples of 400  $\mu\text{l}$  were collected at 1.5 h, 3 h, 4.5 h, 6 h, 7.5 h, 9 h, 22.5 h, 24 h, 25.5 h, 27 h, 28.5 h, 30 h, and 31.5 h from the receptor compartment. The same volume of fresh buffer solution was added after each sampling. NTH concentration was measured by HPLC. Five replicates were performed for each patch.

The cumulative amount of drug permeated through the skin was plotted as a function of time. The diffusion flux at the steady state ( $J$ ,  $\mu\text{g}/(\text{cm}^2 \text{ h})$ ) and lag time were calculated from the slope and intercept of the straight portion of the curve, respectively. The apparent permeability coefficient ( $K_p$ ,  $\text{cm}/\text{h}$ ) was calculated by dividing the flux by the initial concentration in the donor phase and the area of diffusion.

### 2.6. NTH distribution experiments

The penetration profiles have been evaluated for five different films. Three of these patches (A, B and C) were selected as representative of the different combination of the chemical enhancers and the other two patches (P1 and P2) were studied to investigate the effect of drug concentration in the presence and absence of PS80.

#### 2.6.1. NTH distribution within SC

The penetration profile of NTH from the patches within the SC has been evaluated *in vitro* by means of the Saarbrücken (SB) model (Hansen et al., 2008; Jacobi et al., 2005; Wagner et al., 2000, 2004a,b). It consists on an incubation device and a tape-stripping device. For the incubation, a 25 mm diameter piece of skin was put on a filter paper soaked with Ringer solution on a Teflon bloc. The formulation (diameter 13 mm) was placed on the top of the skin and a Teflon punch is fixed over the formulation. The punch has a cavity of 2 mm depth where the formulation remains. The two parts of the device were sealed with Plastibase<sup>®</sup> to avoid water loss from the skin. The whole apparatus was tempered at  $32^{\circ}\text{C}$  in an oven. After the incubation time, the Plastibase<sup>®</sup> was removed with paper cloth and the incubation device was opened. The formulation was completely detached from the skin and the rests of formulation were cleaned with a cotton ball. The skin was then transferred into a special apparatus, where it was fixed with small pins on a cork disc (Wagner et al., 2004a). The skin was covered with a Teflon mask of a 1 cm of diameter hole. The uncovered area was stripped by 20 adhesive tapes under standardized conditions (2 kg pressure for 10 s). It is a critical step of the technique to assure the same contact time and pressure for every strip. The strip was then removed with constant speed and collected in scintillation vials following the sequence:  $S_1$ ,  $S_2$ ,  $S_3$ ,  $S_4$ ,  $S_5$ ,  $S_{6-10}$ ,  $S_{11-15}$ ,  $S_{16-20}$ . NTH was extracted

(see Section 2.6.3) and the drug amount was determined by HPLC. Four replicates were performed for each patch and incubation time.

#### 2.6.2. NTH distribution within DSL

Once the SC was completely removed by stripping, the rest of skin was frozen using expanding carbon dioxide. This technique is fast enough to stop the gradient of diffusion. The skin was placed on a circular piece of aluminum that was fixed in the microtome. The skin was segmented in 25- $\mu\text{m}$  cuts parallel to the surface. Samples were collected in glass tubes by means of a punch. Five sets of samples were defined: incomplete cuts (IC); 2, 2, 2, 2; 4, 4, 4, 4; 8, 8, 8 cuts; and the rest of the skin. NTH was extracted (see Section 2.6.3) and the drug amount was then quantified by HPLC.

#### 2.6.3. Drug extraction of the skin samples

Hydrochloric acid 0.1% was selected as extraction medium. The extraction procedure consists in the addition of 2 ml (stripping samples) or 5 ml (DSL samples) of extraction medium to vials containing the samples. The tubes were maintained for 2 h under slow agitation at room temperature. Afterwards, they were centrifuged and the supernatant was analyzed, after dilution if necessary.

To assure the total recovery, a mass balance was performed. The whole experiment was conducted as usual and every part of the setting up was extracted with the medium, including the rest of formulation applied. After extraction and analysis of all these samples, a mass balance represents the recovery that was established as  $96 \pm 3.7\%$ .

#### 2.6.4. Estimation of SC depth

The whole thickness of the SC has been measured by microscopy of skin cross-sections (Voegeli et al., 2007). Briefly, the method consists of the fixation of skin samples in 4% formaldehyde in PBS (w/v) at room temperature for 4 h. The samples are then dehydrated by exposing them to a graded series of ethanol at 70, 96 and 100% (v/v) at room temperature. They are subsequently placed in xylene for 1 h. After that, the samples were soaked in paraffin at  $60^{\circ}\text{C}$  overnight. 4  $\mu\text{m}$  cuts are obtained with a microtome (Leica Microsystems, Nusslock, Germany) and mounted on glass slides. The samples are cleaned with xylene and rehydrated using ethanol 100, 96 and 70% (v/v). The sections are washed with water and stained with Mayer's haematoxylin solution for 5 min. Afterwards they are cleaned up with tap water for 15 min and counter-stained with Eosin G for 30 s. The samples are washed with 96 and 100% ethanol to remove excess of Eosin G and xylene. Samples were mounted with Histokit<sup>®</sup> (Immunohistochemistry Staining System Peroxidase-based with AEC Chromogen) and examined by CLSM (Karl Zeiss, Jena, Germany) at 1000 $\times$ . With the help of the AxoVision<sup>®</sup> Software the SC thickness can be measured on different cross-sections of the skin. An average of 25 measurements has been taken as reference of the SC thickness of the skin donor.

The thickness of SC removed per strip has been calculated by infrared densitometry using a SquameScanTM<sup>®</sup> 850A device. This device is equipped with a diode which emits light with a wavelength of 850 nm in the infrared range. The reduction in light intensity of each strip can be measured. It is linearly related to the SC density on the tape and is expressed in terms of percentage transmission (%T). The corresponding calibration curve can be used for an indirect evaluation of proteins on tapes. Tape-stripping *in vivo* studies showed a highly significant correlation between %T and the protein content per strip.

#### 2.6.5. Study of the effect of the patch on the stratum corneum at different incubation times by confocal laser scanning microscopy (CLSM)

Skin samples were incubated for 3 h, 6 h and 24 h with the patches. After the incubation time, the formulation was removed

**Table 2**  
Thickness and NTH concentration in the different matrices.

Film	Thickness (mm) (mean ± SD)	C <sub>NTH</sub> (mg/ml) (mean ± SD)	C <sub>NTH</sub> (mg/cm <sup>2</sup> ) (mean ± SD)
A	0.70 ± 0.01	91.6 ± 0.9	115.9 ± 1.7
B	0.68 ± 0.01	104.4 ± 1.6	153.5 ± 3.6
C	0.77 ± 0.03	91.1 ± 5.2	118.3 ± 13.9
D	0.30 ± 0.01	148.4 ± 4.5	494.6 ± 34.6
E	0.25 ± 0.01	215.4 ± 31.3	861.6 ± 564.1

and skin cuts were done. A blank piece of skin was also evaluated for comparison. Skin samples were fixed and prepared as described in Section 2.6.4. After that, photographs were taken.

### 3. Results and discussion

#### 3.1. Physical–chemical properties of the patches

The appearance of the patches was acceptable from the point of view of odour and transparency. A visual inspection of A–D formulations allows considering them as films while formulation E has not an adequate texture. The thickness and NTH content of the different formulations are summarized in Table 2. As it can be seen, the thickness was always lower than 1 mm and showed low variability (coefficient of variation, CV < 4%). NTH content in the matrix was homogeneous (CV < 5.8%) except for formulation E, where the content of NTH was more variable (CV < 14.6%).

Taking into account that initial weight of the gels and the drying conditions were constant, the NTH concentration in patches was expected to be proportional to the initial one. Final concentrations of NTH in the patches are lower than expected when the initial content is increased. This could be explained by a higher retention of solvents in the formed matrix.

#### 3.2. NTH release from the formulations

The parameters estimated by means of the different fittings are summarized in Table 3. Fig. 1 represents the different profiles.

Considering the AIC values, the best model to describe the release kinetics of patches A–D is power law, while patch E release is better fitted by the first order equation. This fact can be explained in light of its different texture due to a lower polymer concentration. In fact, first order kinetics is usually used when the process can be described as dissolution of solid drug and swelling of polymer occurring simultaneously (Capt et al., 2007; Grassi et al., 2007; Korinth et al., 2007).

For comparative purposes, results obtained with the empirical model of power law are reviewed in terms of global effects, as many parameters changed from one formulation to another (thermodynamic activity, solubility, lipid content).

In general, a fickian release can be assumed ( $n$  is estimated between 0.45 and 0.5) as expected due to sink conditions and

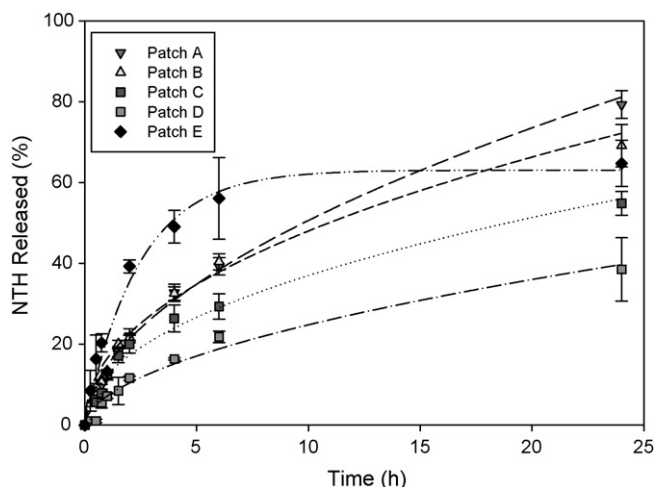


**Fig. 1.** Release profiles for patches A–E. Lines represent the theoretical values calculated by means of the best fit.

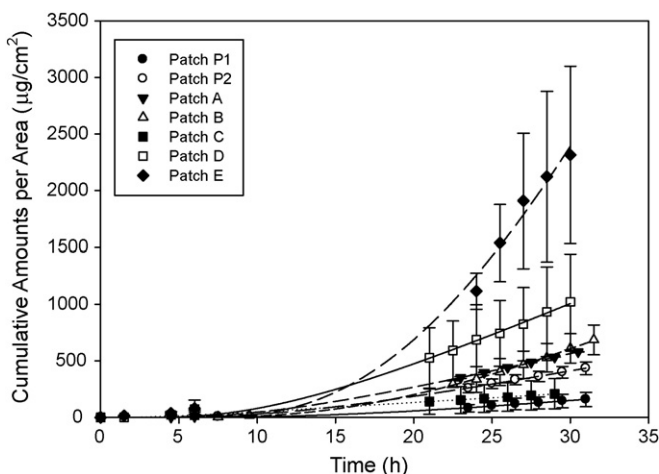


**Fig. 2.** NTH diffusion through HHSE. Results obtained with patches P1 and P2 are represented here for comparison (Melero et al., 2008). Data were fitted by means of the equation described by Scheuplein.

the matrix form (thin film or cylinder). This fact means that mass transport inside the matrix and diffusion occurs mostly in one direction. The release kinetics of patches A and D is characterised by  $n$  slightly higher than 0.5 (statistically different,  $\alpha = 0.05$ ); this could be explained on the basis of boundary conditions. In the case of patch A, the presence of stagnant layers can be produced by the lipid droplets of OA as the patch is free of surfactant. Concerning patch D, the existence of a net faced on the release surface due to the high concentration of NTH could be responsible for it.

**Table 3**  
Release parameters obtained after non-linear regression of different models to data. Figures are presented along with the standard error associated.

Power Law	Film A 4% NTH OA	Film B 4% NTH OA + PS80	Film C 4% NTH PS80	Film D 8% NTH OA + PS80	Film E 10% NTH 1% HPMC OA + PS80
$k_d$ ( $\mu\text{g}/(\text{cm}^2 \text{h})$ )	8.13 ± 0.40	8.84 ± 0.56	7.2 ± 0.50	7.17 ± 0.74	25.03 ± 3.54
$n$	0.54 ± 0.02	0.47 ± 0.02	0.46 ± 0.02	0.54 ± 0.04	0.33 ± 0.06
$r^2$	0.997	0.993	0.991	0.994	0.936
AIC	6.76	7.66	4.26	8.24	18.96
First order	Film A	Film B	Film C	Film D	Film E
$Q_{inf}$	46.54 ± 2.33	39.17 ± 1.83	30.56 ± 2.25	39.35 ± 0.14	63.07 ± 3.06
$K$	0.13 ± 0.01	0.17 ± 0.01	0.18 ± 0.03	0.14 ± 0.01	0.41 ± 0.06
$r^2$	0.993	0.992	0.978	0.986	0.985
AIC	18.80	18.13	17.85	16.46	16.92



**Table 4**  
Diffusion parameters through HHSE. Values are expressed as mean and standard deviation.

	P1 <sup>a</sup> 2% NTH OA	P2 <sup>a</sup> 2% NTH OA + PS80	Film A 4% NTH OA	Film B 4% NTH OA + PS80	Film C 4% NTH PS80	Film D 8% NTH OA + PS80	Film E 10% NTH 1% HPMC OA + PS80
Flux ( $\mu\text{g}/(\text{cm}^2 \text{ h})$ )	$5.80 \pm 2.40$	$14.52 \pm 1.80$	$20.39 \pm 7.09$	$37.21 \pm 9.83$	$7.76 \pm 4.91$	$45.50 \pm 11.9$	$256.19 \pm 94.62$
$K_p \times 10^6$ (cm/s)	$0.023 \pm 0.091$	$0.064 \pm 0.008$	$0.062 \pm 0.006$	$0.099 \pm 0.026$	$0.023 \pm 0.015$	$0.085 \pm 0.049$	$0.341 \pm 0.161$
Lag time (h)	$6.12 \pm 0.65$	$5.63 \pm 0.66$	$3.91 \pm 0.75$	$14.08 \pm 4.97$	$3.59 \pm 1.83$	$5.80 \pm 6.85$	$19.6 \pm 1.99$

<sup>a</sup> From Melero et al. (2008).

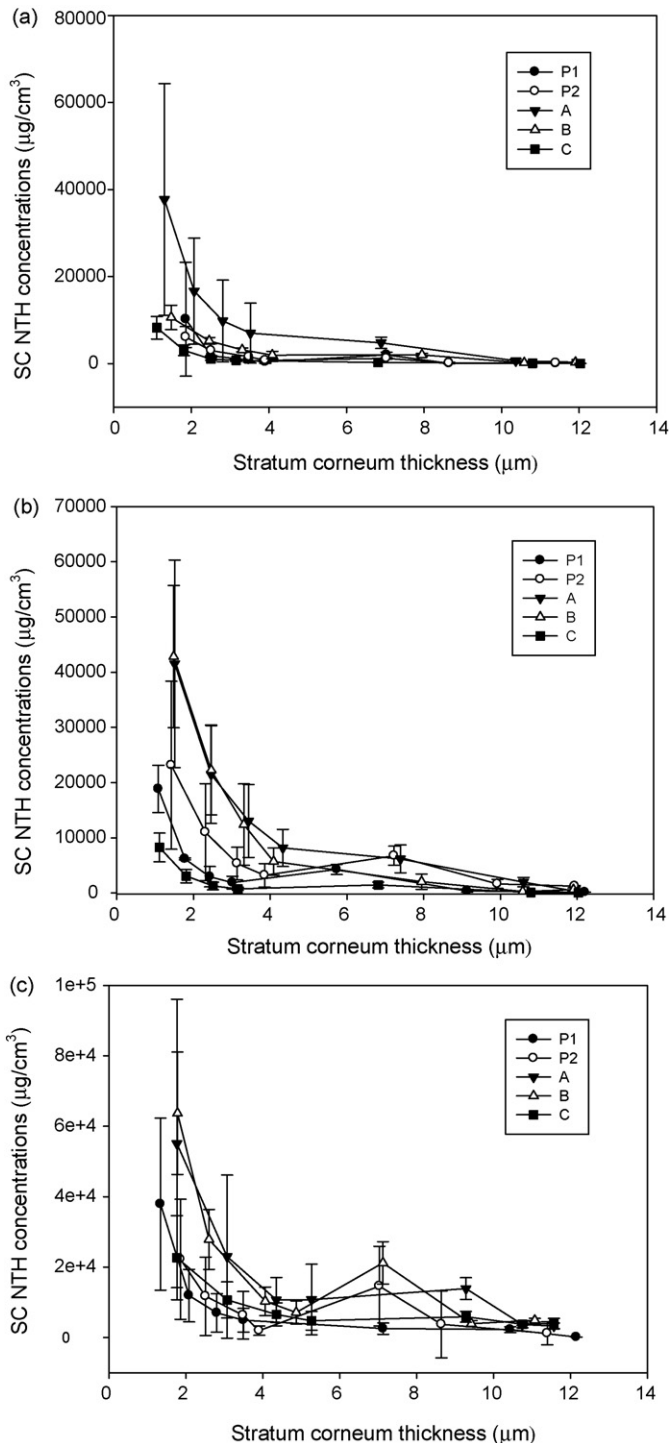


**Fig. 3.** NTH penetration profile (NTH amount per area ( $\mu\text{g}/\text{cm}^2$ ) vs depth) within the SC after 3 h (a), 6 h (b) and 24 h (c) incubation.

On the other hand, OA is able to increase the release rate as seen in the comparison B vs C. The addition of PS80 produces a significant change in the release kinetics (see A vs B), as seen in the exponent.

Concerning the effect of increasing NTH concentration in the patch (B vs D; or P1 and P2 (Melero et al., 2008) vs A and B, respectively), data show a tendency to decrease the rate of release which can be interpreted in light of a retention in the matrix, that is more hydrated as pointed out above (Section 3.1).

### 3.3. NTH diffusion through HHSE

The cumulative amounts of NTH diffused through HHSE at the different sampling intervals have been represented in Fig. 2. In all the experiences, steady state is achieved as can be deduced by the linear portion of the graphs. The calculated parameters, taking this linear part into account, are summarized in Table 4.

Results confirm that there is an increase of the flux when the drug concentration increases in the matrices, as can be observed comparing patches B vs D and E. The fluxes increase but not proportionally, that leads to a bias in the  $K_p$  estimation. The reason for these results could be changes in the network of the gels that led to controlled release.

The most relevant finding is that using PS80 and OA together (film B and D), the highest NTH  $K_p$  value through the skin is achieved (Table 4). This synergistic effect has also been demonstrated by other authors (Williams and Barry, 2004) and reported for many drugs (Gao and Singh, 1998; Yu et al., 1998; Shokri et al., 2001). We can substantiate this affirmation by means of other comparisons. Patch B provides a higher flux and higher  $K_p$  value than A meaning that PS80 alone does not show the same enhancing effect.

Patch C, which does not contain OA, was developed on the basis of previous enhancing experiments of NTH in solution, where the addition of 1% PS80 to a 2% NTH in phosphate buffer solution pH 5.5 provided the highest enhancing activity among all the chemicals

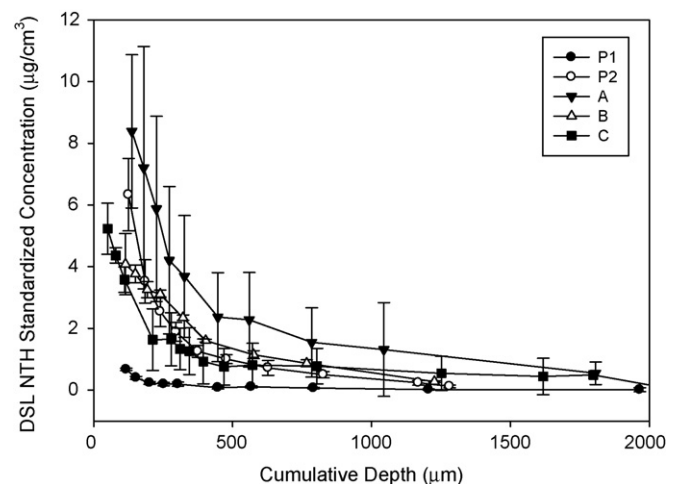


**Fig. 4.** Deeper skin layer profiles from the formulations A–C and P1–P2 after 24 h incubation (mean  $\pm$  SD).

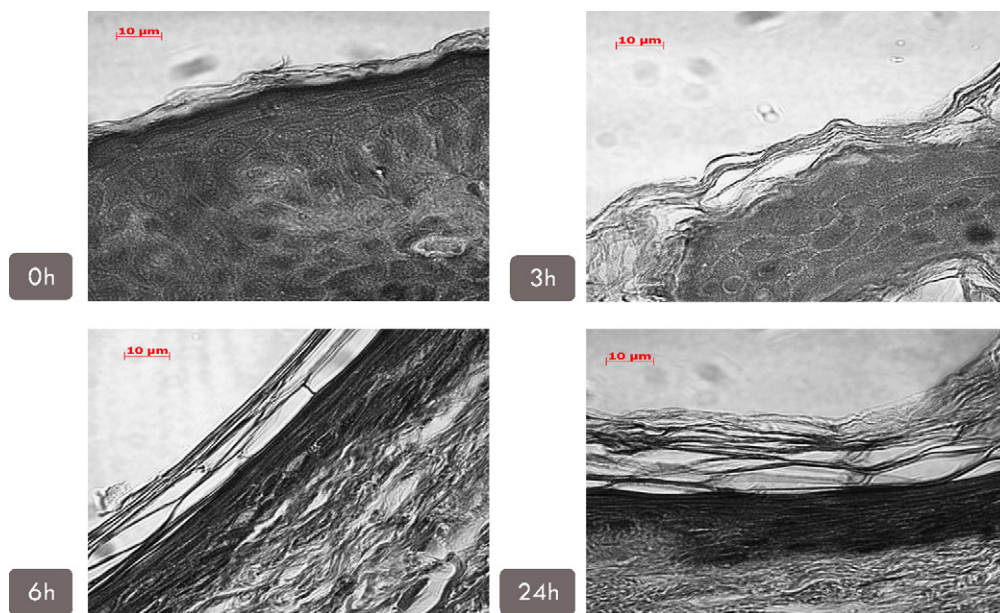


Fig. 5. CLSM photographs of skin cross-section after 0 h, 3 h, 6 h and 24 h incubation with patch B.

tried (Melero et al., 2008). But the comparison of C vs B patches to test the OA effect, gives an enhancement about 4.3.

### 3.4. NTH distribution within the skin layers

#### 3.4.1. Stratum corneum

The influence of the incubation time on the NTH penetration profile can be evaluated in Fig. 3 where the amount of NTH is represented for the five patches studied as a function of the SC thickness. It can be seen that the amount of drug decreases with SC depth for each incubation time. This tendency is in accordance with Fick's law of diffusion and the literature (Wagner et al., 2000; Lademann et al., 2009). The amount of drug permeated increases for all formulations when increasing the incubation time, as it was expected.

Comparing the five different vehicles, after 3 h and 6 h (Fig. 3a and b), patch A seems to be the best because the highest amounts of NTH are found in the SC. Nevertheless, after 24 h (Fig. 3c), patch B provides the highest amounts of drug. This fact is in agreement with data obtained from FDC experiments that demonstrated a higher lag time for patch B than for patch A (see Table 4). An explanation could be that PS80, present in patch B, would form micelles able to initially retard the release of the other enhancers but once the process is in progress, the combination of them would better enhance the pass of the drug through the SC, the limiting barrier. Another possibility is that PS80 would disrupt the corneocytes or diminish the consistence of the lipid membrane structure in a more efficient way but needing a longer period of time to develop the action. The enhancing effect of OA is obvious considering that patch C (containing double amount of NTH but no OA) provides a less effective penetration of drug than patch P2. The influence of the increase of drug concentration of the patches in NTH penetration though the SC can also be seen in these experiments by comparison of patches P1 vs A and P2 vs B, showing an increase in the final NTH amount, as it was expected.

#### 3.4.2. Deeper skin layers (viable epidermis and dermis)

DSL samples after 3 h and 6 h of incubation time presented drug amounts below the quantification limit of the analytical method. After 24 h incubation, a diffusion gradient into the DSL was achieved and a penetration profile was described as shown in Fig. 4. The diffusion is very low for patch P1 and the highest amounts of NTH

are found for patch B, in correspondence to the results obtained from the SC and the FDC experiments.

Patch P2 provides a similar profile than patch A containing half the amount of drug. This fact suggests that the enhancing effect of PS80 also affects the gradient of diffusion of NTH through the DSL.

Surprisingly, the profile of DSL for patch C is similar to the ones obtained for P2 and A, while it was slower after the other types of experiences. It can be observed that the effect of PS80 and OA in the penetration of NTH through DSL seems very similar (P2 vs C), and the combination of both enhancers (patch B) produces the highest enhancement.

#### 3.4.3. Evaluation of the changes in the SC after 3 h, 6 h and 24 h incubation by CLSM

The photographs of skin samples treated as described in Section 2.6.4 allow a comparison of the effects of the incubation time on the corneocytes size. As can be observed in Fig. 5, there is a time-dependent increase of their size. This could be explained by occlusion of the skin under the patches that would lead to a migration of water from the deeper skin layers to the SC. The occlusion effect has been previously reported (Trommer and Neubert, 2006) and shows the water as penetration enhancer, as the cohesion of corneocytes is altered and therefore the diffusion of drug enhanced.

## 4. Conclusions

On the basis of these results, it can be concluded that NTH can be administered via the skin by HPMC patches. Release of the drug is extended over a long period of time. NTH diffusion through human skin can be modulated by addition of EtOH, PG and PS80 combined with the occlusion effect of the formulation by itself. The best result is obtained by the synergistic effect of OA plus PS80.

Taking into account that the daily oral dose of NTH for smoking cessation therapy is 25 mg in the first step of the treatment and 75 mg in the second step, and its bioavailability is between 30 and 50%, patches B and D would provide the needed amount of NTH. Patch B needs a size of 3 cm × 3 cm for the first therapy and a size of 5 cm × 5 cm for the second step of the therapy. Patch D needs a size of 2.6 cm × 2.6 cm and 4.5 cm × 4.5 cm, respectively and its lag time is significantly lower.

Animal studies should be carried out to assess these results before going into clinical trials.

## Acknowledgments

The authors would like to thank the DAAD grant for A. Melero, the Galenos Network-Marie Curie-Fellowship agreement in the framework of the EU Project “Towards a European Ph.D. in Advanced Drug Delivery” MEST-CT-2004-504992, the project FIS Instituto de Salud San Carlos III FI 060944 (953/2006) and Professors Adela Martin-Villodre and Marina Herraes for their help on the discussion of the results.

## References

- Capt, A., Luzy, A.P., Esdaile, D., Blanck, O., 2007. Comparison of the human skin grafted onto nude mouse model with in vivo and in vitro models in the prediction of percutaneous penetration of three lipophilic pesticides. *Regul. Toxicol. Pharmacol.* 47, 274–287.
- Dragevic-Ciric, N., Scheglmann, D., Albrecht, V., Fahr, A., 2009. Development of different temoporfin-loaded invasomes—novel nanocarriers of temoporfin: characterization, stability and in vitro skin penetration studies. *Colloids Surf. B: Biointerface* 70, 198–206.
- Farahmand, S., Maibach, H.I., 2009. Transdermal drug pharmacokinetics in man: interindividual variability and partial prediction. *Int. J. Pharm.* 367, 1–15.
- Gao, S., Singh, J., 1998. Effect of oleic acid/ethanol and oleic acid/propylene glycol on the in vitro percutaneous absorption of 5-fluorouracil and tamoxifen and the macroscopic barrier property of porcine epidermis. *Int. J. Pharm.* 165, 45–55.
- Ghahramani, P., Lennard, M.S., 1996. Quantitative analysis of amitriptyline and nortriptyline in human plasma and liver microsomal preparations by high-performance liquid chromatography. *J. Chromatogr. B: Biomed. Appl.* 685, 307–313.
- Grassi, M., Lapsin, R., Colombo, I., 2007. *Understanding Drug Release and Absorption Mechanisms. A Physical and Mathematical Approach*. CRC Press, Boca Raton (FL), 648 pp.
- Hansen, S., Henning, A., Naegel, A., Heisig, M., Wittum, G., Neumann, D., Kostka, K.H., Zbytovska, J., Lehr, C.M., Schaefer, U.F., 2008. In-silico model of skin penetration based on experimentally determined input parameters. Part I. Experimental determination of partition and diffusion coefficients. *Eur. J. Pharm. Biopharm.* 68, 352–367.
- Jacobi, U., Taube, H., Schaefer, U.F., Sterry, W., Lademann, J., 2005. Comparison of four different in vitro systems to study the reservoir capacity of the stratum corneum. *J. Control. Release* 103, 61–71.
- Kligman, A.M., Christophers, E., 1963. Preparation of isolated sheets of human stratum corneum. *Arch. Dermatol.* 88, 702–705.
- Korinath, G., Goen, T., Schaller, K.H., Drexler, H., 2007. Discrepancies between different rat models for the assessment of percutaneous penetration of hazardous substances. *Arch. Toxicol.* 81, 833–840.
- Lademann, J., Jacobi, U., Surber, C., Weigmann, H.J., Fluhr, J., 2009. The tape stripping procedure—evaluation of some critical parameters. *Eur. J. Pharm. Biopharm.* 72, 317–323.
- Melero, A., Garrigues, T.M., Almudever, P., Martin-Villodre, A., Lehr, C.M., Schäfer, U., 2008. Nortriptyline Hydrochloride skin absorption: development of a transdermal patch. *Eur. J. Pharm. Biopharm.* 69, 588–596.
- Morris, A.P., Brain, K.R., Heard, C.M., 2009. Skin permeation and ex vivo skin metabolism of o-acyl haloperidol ester prodrugs. *Int. J. Pharm.* 367, 44–50.
- Prohazka, A.V., Keller, W.M., Fryer, R.T., Licari, G.E., Lofaso, P.A., 1998. A randomized trial of Nortriptyline for smoking cessation. *Arch. Intern. Med.* 158, 2035–2039.
- Shokri, J., Nokhodchi, A., Dashbolaghi, A., Hassan-Zadeh, D., Ghafourian, T.M., Barzegar-Jalali, M., 2001. The effect of surfactants on the skin penetration of diazepam. *Int. J. Pharm.* 228, 99–107.
- Siepmann, J., Peppas, N.A., 2001. Modeling of drug release from delivery systems based on hydroxypropyl methylcellulose (HPMC). *Adv. Drug Deliv.* 48, 139–157.
- Stimmel, G.L., 1996. Benzodiazepines in schizophrenia. *Pharmacotherapy* 16, 148S–151S (discussion 166S–168S).
- Trommer, H., Neubert, R.H., 2006. Overcoming the stratum corneum: the modulation of skin penetration. A review. *Skin Pharmacol. Physiol.* 19, 106–121.
- Voegeli, R., Heiland, J., Doppler, S., Rawlings, A.V., Schreier, T., 2007. Efficient and simple quantification of stratum corneum proteins on tape strippings by infrared densitometry. *Skin Res. Technol.* 13, 242–251.
- Wagner, H., Kostka, K.H., Lehr, C.M., Schaefer, U.F., 2000. Drug distribution in human skin using two different in vitro test systems: comparison with in vivo data. *Pharm. Res.* 17, 1475–1481.
- Wagner, H., Zghoul, N., Lehr, C.M., Schaefer, U.F., 2004a. In-vitro Test Systems for Drug Absorption and Delivery. Book Chapter 17: Human Skin and Skin Equivalents to Study Dermal Penetration and Permeation. Taylor and Francis, London, New York.
- Wagner, H., Kostka, K.H., Adelhardt, W., Schaefer, U.F., 2004b. Effects of various vehicles on the penetration of flufenamic acid into human skin. *Eur. J. Pharm. Biopharm.* 58, 121–129.
- Williams, A.C., Barry, B.W., 2004. Penetration enhancers. *Adv. Drug Deliv. Rev.* 56, 603–618.
- Yu, D., Sanders, L.M., Davidson, G.W., Marvin III, M.J., Ling, T., 1998. Percutaneous absorption of nicardipine and ketorolac in rhesus monkeys. *Pharm. Res.* 5, 457–462.